Molecular Crystals and Liquid Crystals

ISSN: 1542-1406 (Print) 1563-5287 (Online) Journal homepage: http://www.tandfonline.com/loi/gmcl20

Evolution of Microwave Nematic Liquid Crystal Mixtures and Development of Continuously Tuneable Micro- and Millimetre Wave Components

M. Jost, A. Gaebler, C. Weickhmann, S. Strunck, W. Hu, O. H. Karabey & R. Jakoby

To cite this article: M. Jost, A. Gaebler, C. Weickhmann, S. Strunck, W. Hu, O. H. Karabey & R. Jakoby (2015) Evolution of Microwave Nematic Liquid Crystal Mixtures and Development of Continuously Tuneable Micro- and Millimetre Wave Components, Molecular Crystals and Liquid Crystals, 610:1, 173-186, DOI: 10.1080/15421406.2015.1025645

To link to this article: http://dx.doi.org/10.1080/15421406.2015.1025645

Published online: 06 Jul 2015.

Mol. Cryst. Liq. Cryst., Vol. 610: pp. 173–186, 2015

ISSN: 1542-1406 print/1563-5287 online
DOI: 10.1080/15421406.2015.1025645

Taylor & Francis
Taylor & Francis Group

Evolution of Microwave Nematic Liquid Crystal Mixtures and Development of Continuously Tuneable Micro- and Millimetre Wave Components

M. JOST,* A. GAEBLER, C. WEICKHMANN, S. STRUNCK, W. HU, O. H. KARABEY, AND R. JAKOBY

Institute for Microwave Engineering and Photonics, Technische Universität Darmstadt, Darmstadt, Germany

This work represents the evolution of micro- and millimetre wave optimized nematic liquid crystal mixtures and their applications. Starting with the well-known liquid crystal mixture K15 used in the display technology, microwave optimized LC mixtures have been developed. For that, novel characterization setups have been developed, which play an essential factor in the optimization process for the micro-, millimetre wave and THz regime. By using a specialized LC simulation tool, different tuneable waveguide topologies are compared in terms of tuneability, transmission loss and tuning speed. Based on that, a phase shifter for W-band frequencies has been fabricated, which reached a measured figure of merit for passive phase shifters of up to 148° /dB.

Keywords Liquid Crystal; Tuneable Material; Characterisation; Simulation; Phase Shifter; Millimetre Wave

Introduction

During the last decade, calamitic-nematic liquid crystals (LCs), well-known from the LC-display technology (LCD) [1], have become increasingly popular in the field of microwave engineering. LC mixtures are fluid like liquids while having properties similar to a crystalline phase. The molecules are uniaxial anisotropic materials featuring different polarization depending on the orientation to an applied radio frequency (RF) field, resulting in different macroscopic permittivities. The orientation of LC can be controlled by almost electrostatic or magneto-static fields, that is known as the Fréedericksz transitions [2]. One of the first attempts to open up the field of LC towards the microwave range was made in 1993 [3], while one of the first attempts of our group was done in 2002 [4]. After the first experiments in our group were carried out using the well-known display LC K15, it quickly became clear that this LC is not optimized for the microwave range. The figure of merit

*Address correspondence to M. Jost, Institute for Microwave Engineering and Photonics, Technische Universitaet Darmstadt, Merckstr. 25, Darmstadt, Germany 64283. E-mail: jost@imp.tu-darmstadt.de

Color versions of one or more of the figures in the article can be found online at www.tandfonline.com/gmcl.

(FoM) for passive phase shifters is defined as

$$FoM = \frac{\Delta\varphi_{\max}}{IL_{\max}}\,[^\circ/\mathrm{dB}]\,. \tag{1}$$

There, $\Delta\varphi_{\max}$ is the maximum differential phase shift, while $IL_{\max}$ is the maximum insertion loss of the device. For this first LC-based phase shifter, the *FoM* was low (12° /dB at 18 GHz [4]) compared to other technologies, e.g. MEMS (154° /dB at 25 GHz [5]).

In order to optimize the LC mixtures for the microwave regime, a variety of characterisation methods have been developed allowing the dielectric properties of the mixtures to be determined. There are two main characterisation methods, one, which is the transmission line approach, is broadband. The other one is a narrowband resonator approach, based on the cavity perturbation theory. Examples for broadband characterizations are the temperature controlled artificial coaxial line setup, built up for frequencies from 360 MHz to 23 GHz [6] as well as a hollow-waveguide-based characterisation setup for W-band frequencies [7]. Furthermore narrow-band resonator-based setups have been implemented, which are based on the cavity perturbation theory [8, 9]. However, these measurements provide more accurate results than the broadband measurements, but only at a single frequency. The latest setup is based on a cylindrical resonator, which provides a higher accuracy than rectangular resonators shown in [9]. In this work we will focus on the resonator based characterisation setups. For the broadband methods we refer to [6, 7].

With the help of these characterisation setups, the LC mixtures could be improved in cooperation with Merck KGaA, Darmstadt, which led to a loss reduction by a factor of 5 ($\tan\delta = 0.006$). This is an excellent value for tuneable dielectric materials in the microwave range, which is close to the value of typical commercial substrates like ROGERS. The dielectric properties of certain LCs were measured up to 1.5 THz using a time-domain spectroscopy (TDS) system, which suggests a nearly constant dielectric behaviour [10].

The material dependent parameters have been used to investigate the behaviour of different tuneable waveguide topologies with the help of an in-house simulation tool called *SimLCwg* [11]. In particular the coplanar waveguide (CPW), the inverted microstrip line (IMSL) and the hollow waveguide are investigated in this work. *SimLCwg* calculates not only the RF modes of a structure but also the LC alignment with respect to an electrostatic biasing field or a prealignment at LC cavity borders. The line impedance, transmission loss and tuneability can be obtained from these simulations. The inverted microstrip line exceeds the coplanar waveguide and other planar structured waveguides in terms of tuneability and phase shifter figure of merit. However, the calculations also show that the hollow waveguide topology is the best solution for high performance phase shifters, due to lower metallic losses.

Because of these results, LC-based devices, such as phase shifters, can be separated in two different categories, the planar structured devices (e.g. for mobile communication in cars or aircrafts) based on low-profile transmission lines and the high performance devices (e.g. for satellite communication) based on hollow-waveguides. While the advantage of a hollow-waveguide based LC device is its high FoM, the planar structures benefit from a low response time of the LC due to comparatively thin LC layer thicknesses. The response time depends on d^2, where d is the LC layer thickness. While the best *FoM* for planar structured LC phase shifters in our group was 110° /dB [12], a record *FoM* of 200° /dB was achieved using a hollow-waveguide based LC phase shifter [13].

Over the years, many passive, tuneable microwave components based on LC have been developed, such as filters [14] and phased array antennas for satellite communication [15],

reconfigurable reflectarray antennas for radar applications [16], low profile phased array antennas for mobile communication [17], polarization agile antennas or hollow-waveguide based polarizers for polarization dependent channel separation in satellite communications or synthetic aperture radar (SAR) application [18, 19].

One application, an LC based low-loss hollow waveguide phase shifter for frequencies from 80 GHz to 110 GHz, will be presented. This demonstrator is biased using permanent magnets as a first proof-of-concept, showing the compatibility of LC for W-band applications. An FoM between 108° /dB to 148° /dB is reached, which is, to the authors' knowledge, the highest value for passive phase shifters in this frequency range to date.

Properties of Liquid Crystal

Calamitic-nematic liquid crystals exist in a phase between an isotropic liquid and a crystalline solid. The molecules can be illustrated as rod-like shapes. They tend to align parallel to each other along a preferred direction, resulting in an uniaxial anisotropic material. The average molecular alignment of a unit volume of LC can be described by defining a macroscopic unit vector $\boldsymbol{n}$, which is called the director (see Figure 1). Due to the high dielectric anisotropy, the polarization along the director differs from the polarization orthogonal to it, which means that the effective relative permittivity $\varepsilon_{r,\text{eff}}$ and dielectric losses $\tan\delta$ of the LC depend on the orientation with respect to the applied RF field. The two extreme states for this are parallel $\left(\varepsilon_{r,\text{eff}} = \varepsilon_{\parallel}\right)$ or perpendicular $\left(\varepsilon_{r,\text{eff}} = \varepsilon_{\perp}\right)$ to the RF field, between which the LC can be oriented continuously $\left(\varepsilon_{\perp} < \varepsilon_{r,\text{eff}} < \varepsilon_{\parallel}\right)$.

The orientation of the director $\boldsymbol{n}$ can be influenced in three different ways. First by covering the LC-cavity-substrate with an alignment layer, which anchors the rod-like shaped LC molecules at the surface parallel to the electrodes. Second, an applied chopped electrostatic or third a magneto-static field, both orient $\boldsymbol{n}$ of the LC molecules parallel to its field lines. However, magneto-static fields are only used in the laboratory for characterisation purposes, because orientation requires strong magnetic fields, usually between 0.2 to 0.7 Tesla. Thus, this orientation mechanism is not reasonable for practical applications up to now. For tuning microwave components with a chopped electrostatic fields, several pairs (3 to 7) of electrodes are required to change the direction and strength of the field inside the device [13, 20]. The electrostatic field needs to be chopped, otherwise it would damage the LC structure.

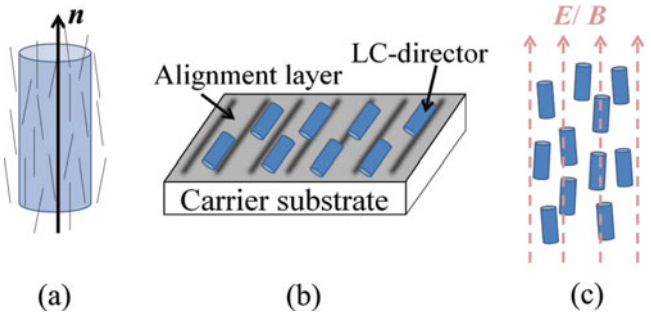

Figure 1. (a) Individual LC molecules and their macroscopic director (cylinder) $\boldsymbol{n}$, (b) LC directors oriented along an alignment layer on a carrier substrate and (c) LC directors oriented by an external magnetostatic/ chopped electrostatic field.

Based on the aforementioned dielectric properties, the material tuneability τ_{LC} is given by

$$\tau_{\mathrm{LC}} = \frac{(\varepsilon_{\parallel} - \varepsilon_{\perp})}{\varepsilon_{\parallel}}. \tag{2}$$

It quantifies the anisotropy of the LC. Combined with the maximum dielectric loss $\tan\delta_{max}$ of the material, the material quality factor

$$\eta_{\mathrm{LC}} = \frac{\tau_{\mathrm{LC}}}{\tan\delta_{\mathrm{max}}} \tag{3}$$

is defined. The properties of the LCs used in this work are shown in Table 1.

Characterisation of Liquid Crystal

The dielectric properties shown in Table 1 can either be determined using a transmission line-/ waveguide-based broadband characterisation setup [6, 7] or by using a resonator-based setup, which uses the cavity perturbation technique. There, a resonator equipped with a sample holder will be measured with and without a dielectric filling of the sample holder. The dielectric filling will result in a shift of the resonant frequency compared to the empty measurement, from which the dielectric properties of the material can be calculated. While this kind of measurement is limited to a single frequency, the dielectric properties and especially the dielectric loss can be determined much more precise than with broadband measurement setups, due to the high quality factor of the resonator. A first setup is shown in [8]. While only one orientation of the LC can be evaluated in one measurement step with this setup, a second setup was investigated, with which it is possible to determine both axes of the complex LC-permittivity temperature dependent in one measurement step by using a rectangular resonator, thanks to the triple-mode cavity perturbation method [9]. This resonator is designed to allow the occurrence of three orthogonal modes, each of them having only one E-field component in x, y or z direction respectively. Therefore all needed material parameters can be extracted in one single measurement.

Since two of these three modes lead to the same results - the dielectric properties of the perpendicular LC orientation - a dual-mode cylindrical resonator is designed. With this resonator, all needed parameters can be measured as well and further the quality factor of the cylindrical resonator is higher than the one of the rectangular resonator, which leads to an even higher accuracy. The resonator and a schematic of the used modes are shown in Figure 2.

A sample holder (glass-tube) is placed in the centre of a cylindrical resonator. The excitation is provided through a circular opening just above the bottom plate of the resonator,

Table 1. Dielectric properties of different LC mixtures used in this work measured at 19 GHz and room temperature (courtesy of Merck KGaA, Darmstadt)

LC	$\varepsilon_{\perp}$	$\tan\delta_{\perp}$	$\varepsilon_{\parallel}$	$\tan\delta_{\parallel}$	$\tau_{\mathbf{LC}}$	$\eta_{\mathbf{LC}}$
K15	2.65	0.025	2.95	0.01	0.102	4.1
GT3-23001	2.46	0.0143	3.28	0.0038	0.252	17.6
TUD-566	2.41	0.006	3.34	0.0027	0.280	46.0
TUD-126	2.39	0.007	3.27	0.0022	0.270	38.3

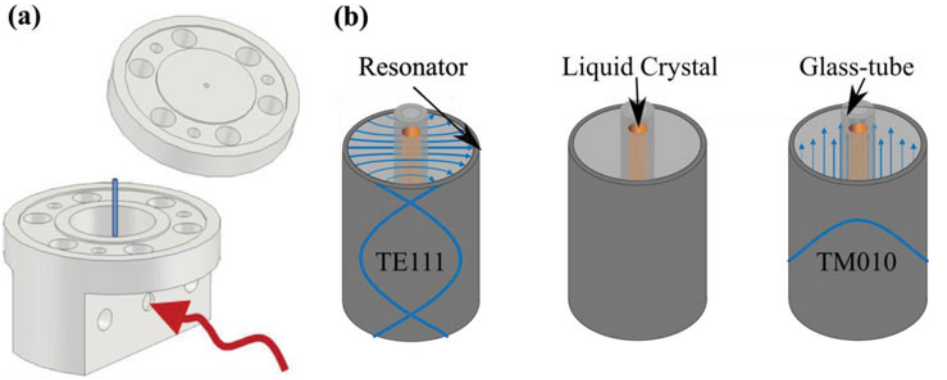

Figure 2. Schematic of (a) the resonator including the glass-tube sample holder and (b) the cavity itself including the glass-tube sample holder, the liquid crystal and the RF-modes.

which is fed by a rectangular waveguide. Two different modes will be evaluated, each of them having an electric field distribution only parallel or perpendicular to the long axis of the glass-tube respectively. Therefore, both axes of the LC permittivity can be determined in one measurement step. The orientation of the LC during the measurements will be fixed with the help of permanent magnets.

For this purpose, a differential measurement method is chosen, where measurements with empty and filled sample holder will be compared and evaluated. Due to the dielectric properties of the LC, the field distribution and therefore the resonance frequency of the propagating mode will shift compared to the measurement with an empty glass tube. Systematic measurement errors can be reduced by that.

In the following, the field equations for a cylindrical cavity with a three-layered lossless anisotropic dielectric material (LC, glass and air) are derived, which is surrounded by a perfect electric conductor (PEC). The dielectric material is assumed to be homogenous. The approach are the wave equations in cylindrical coordinates

$$\left(\frac{d}{d\rho^2}+\frac{1}{\rho}\frac{d}{d\rho}+\frac{1}{\rho^2}\frac{d}{d\varphi^2}\right)E_z+k_c^2E_z=0 \tag{4}$$

$$\left(\frac{d}{d\rho^2}+\frac{1}{\rho}\frac{d}{d\rho}+\frac{1}{\rho^2}\frac{d}{d\varphi^2}\right)H_z+k_c^2H_z=0, \tag{5}$$

whose general solutions are known as

$$\Phi_H(\varphi)=H_0\cdot e^{im\varphi} \tag{6}$$

$$\Phi_E(\varphi)=E_0\cdot e^{im\varphi} \tag{7}$$

$$P_H(\rho)=A\cdot J_m(k_h\cdot\rho)+B\cdot N_m(k_h\cdot\rho) \tag{8}$$

$$P_E(\rho)=C\cdot J_m(k_e\cdot\rho)+D\cdot N_m(k_e\cdot\rho), \tag{9}$$

with $E_z(\rho,\varphi)=P_E(\rho)\cdot\Phi_E(\varphi)$ and $H_z(\rho,\varphi)=P_H(\rho)\cdot\Phi_H(\varphi)$. The arguments k_h and k_e of the m$^{\text{th}}$-order Bessel- (J) and Neumann-functions (N) are $k_h^2=\omega^2\varepsilon_{\text{transv.}}\mu-\beta^2$ and $k_e^2=\frac{\varepsilon_{\text{long.}}}{\varepsilon_{\text{transv.}}}(\omega^2\varepsilon_{\text{transv.}}\mu-\beta^2)$. Using Maxwell's equations, the transversal field components can be solved only with the help of the longitudinal field components.

The unknown amplitudes A, B, C and D can be determined employing the continuity conditions of the tangential E- and H-field components present at the interface. For this, the transversal and longitudinal field components have to be equated and the resulting system of equations, which includes six unknown parameters and six equations, needs to be solved. The dielectric properties of the material can thus be determined, if the geometric dimensions and the propagation constant are known. Because of the known resonator dimensions, the propagation constant is given by $\beta = \frac{2\pi}{\lambda} = \frac{\pi}{h}$ for the TE111-mode and $\beta = 0$ for the TM010-mode respectively.

The dielectric loss is obtained by determination of the complex permittivity using a complex propagation constant. The field distribution obtained in this way is no longer the exact solution of Maxwell's equations. Nevertheless, the disagreement with the exact calculations according to [21] is negligible, if the effect of the dielectric losses on the RF field are small, as it is the case in all previously investigated LC mixtures ($\tan\delta_{max} < 0.04$).

The electric field of the quasi TM010-mode only has a z-component at the resonance frequency, even after the disturbance due to the dielectric material. It is therefore reasonable to determine the permittivity of the long LC-axis first by solving the system of equations for $m = \beta = 0$. Due to the fact that the LC influences the RF field because of its higher permittivity, the Brent-Dekker method [22] needs to be used for the exact determination of the permittivity. Afterwards the permittivity of the short LC-axis can be determined in a similar way by considering the TE111-mode.

This kind of an analytical solution is only valid and exact for geometrically simple structures and a perfectly electric conducting surrounding without any coupling- or sample-insertion-holes. In this regard, the method takes advantage of the differential measurement method. However, since both the resonant frequency and the field distribution depend on the dielectric filling of the cavity, the effects are not taken into account by now in both measurements. If the field is known and the yet unrecognized factors sufficiently small, they can be treated as perturbations and determined by approximate computation. For this purpose the influence of three different perturbations is investigated, which are the interference of the incident and scattered electric field at the sample-insertion-holes, the finite conductivity of the surrounding cavity, which can be determined with the help of the "Power Loss-method", and the perturbation due to the coupling-holes. The coupling-holes have the lowest influence on the material characterisation, because of the low field-distortions at the edges due to a centred sample. This leads to an improvement of the model underlying the characterisation and thus to a more accurate determination of the material parameters. Further, the additional systematic errors can be estimated.

By providing this characterisation method, the LC mixtures could be improved for the micro- and millimetre wave range in cooperation with Merck KGaA, Darmstadt. A comparison of different LCs, measured at 19 GHz and room temperature, is shown in Figure 3. The values for $\tan\delta$ were reduced by a factor of 5 from K15 to TUD-566 as well as the tuneability was increased almost by a factor of 3. With the GT3-23001 mixture, Merck launched the first commercial microwave-optimized LC mixture.

As one advantage of LC is the decreasing dielectric loss with increasing frequency in the lower GHz range, measurements up to 1.5 THz have been carried out using a time-domain spectroscopy THz measurement system [10]. One of the characterized LC was the GT3-23001 mixture, which shows an almost constant permittivity over a wide frequency range between 200 GHz to 1.5 THz. The values $\varepsilon_\perp = 2.34$ and $\varepsilon_\parallel = 3.19$ fit well (5.1 % deviation for the perpendicular state and 2.8 % for the parallel state) with the reference values from Merck at 19 GHz (see Table 1). These are promising results for LC to be a well suited tuneable material for reconfigureable devices in the millimetre wave and THz regime.

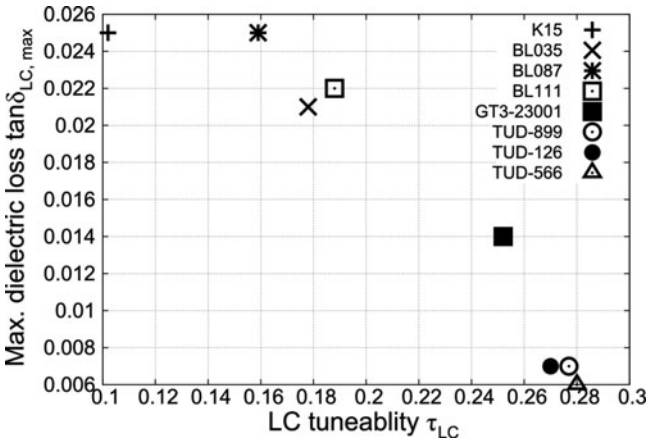

Figure 3. Comparison of LC tuneability and maximum dielectric loss of different LC mixtures, measured with the characterisation method mentioned above at 19 GHz.

Director Dynamics Simulation (*SimLCwg*)

The material parameters obtained in this way are for example used to simulate the behaviour of LC-based devices, inter alia with our in-house simulation tool *SimLCwg* [23, 24]. As an example, an LC-based microstrip line phase shifter is investigated. To determine the behaviour of LC-filled transmission lines, it is necessary to consider the inhomogeneous and fully anisotropic properties as well as the director dynamics in these structures. If the LC is not aligned parallel to one of the walls but somewhere in between, the electrical flux density $\boldsymbol{D}$ is not parallel to the incident electrical field $\boldsymbol{E}$ anymore, and therefore, all entries of the permittivity-matrix have to be considered, because the E-field is changing due to the anisotropic filling of the waveguide. If the LC is oriented parallel to any axis of the chosen coordinate system, all non-diagonal matrix elements are equal to zero.

Starting point for the simulation of time-dependent orientation processes of LC directors is the continuum theory developed by Frank and Oseen [25, 26]. The free energy stored in a bulk of LC-molecules is a function of its dielectric and elastic constants. It causes locally effective torques, which are shown in Figure 4.

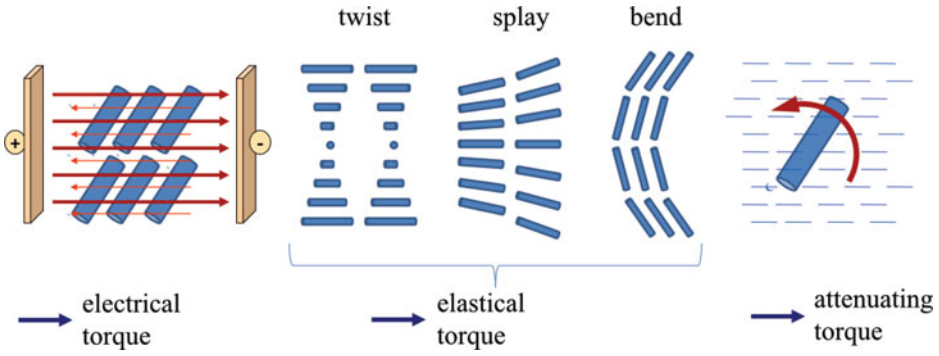

Figure 4. Considered contributions of the free energy and the dissipative momentum.

The dissipative momentum counteracts the movement of the LCs caused by the free energy and its magnitude depends on the rotational viscosity γ_{rot}. Thus the torque-balance-equation

$$\Gamma_{\mathrm{electr}} + \Gamma_{\mathrm{elast}} + \Gamma_{\mathrm{diss}} = 0 \tag{10}$$

is composed of the electrical torque

$$\Gamma_{\mathrm{electr}} = \frac{1}{2} \cdot \Delta\varepsilon \cdot \varepsilon_0 \cdot |E| \cdot sin\,(2 \cdot \beta)\,, \tag{11}$$

the elastic torque

$$\Gamma_{\mathrm{elast}} = \frac{\partial f}{\partial n_i} - \left(\frac{d}{dx} \frac{\partial f}{\partial \left(\frac{dn_i}{dx}\right)} + \frac{d}{dz} \frac{\partial f}{\partial \left(\frac{dn_i}{dz}\right)} \right) \tag{12}$$

and the dissipative torque

$$\Gamma_{\mathrm{diss}} = -\gamma_{\mathrm{rot}} \frac{\partial \varphi}{\partial t}. \tag{13}$$

The angle β is the angle between the applied electric field and the LC director $\boldsymbol{n}$. The elastic torque is derived by the stored free energy density of a LC bulk, which can be described by the Frank free energy density

$$f = \frac{1}{2} K_{11} (\nabla \cdot \boldsymbol{n})^2 + \frac{1}{2} K_{22} \left(\boldsymbol{n} \cdot \nabla \times \boldsymbol{n}^2\right)^2 + \frac{1}{2} K_{33} \cdot (\boldsymbol{n} \times \nabla \times \boldsymbol{n})\,. \tag{14}$$

For modeling different LCs, the elastic constants for twist (K_{11}), splay (K_{22}) and bend (K_{33}) are considered. Regarding the minimum energy principle, the free energy can be minimized using the Lagrange principle, which results in the equation for the elastic torque shown above. The dissipative torque originates from the internal friction which occurs due to a movement of the director towards the minimum energy level, caused by an imbalance of the electrical and elastic torques. The solution of the torque-balance equation leads to a director update formulation for discrete time steps Δt and results in an iterative solving of the energy minimizing problem. If the director distribution does not change in two subsequent time steps, it is assumed that the simulation has calculated a stable bias condition and therefore the minimum energy level is reached.

A flow chart of a director update calculation for an inverted microstrip line (IMSL) is shown in Figure 5. It shows the time needed for a LC alignment from perpendicular to parallel using a chopped electrostatic field. The re-alignment due to the alignment layer is presented as well, which begins after switching off the voltage of the electrostatic field. Based on the director field on the bottom of Figure 5, the LC directors start to turn back quickly. The restoring force and thus the re-aligning speed slow down steadily with decreasing elastic deformations in the LC volume until the starting condition (perpendicular state) is almost reached again. The re-alignment using the alignment layer needs more time than the alignment using the biasing electrodes. After the director distribution reached its minimum energy level, the RF eigenmodes can be calculated as well.

In this way different transmission line and hollow waveguide based LC phase shifters can be assessed in terms of their tuneability, figure of merit or tuning speed. The tuning

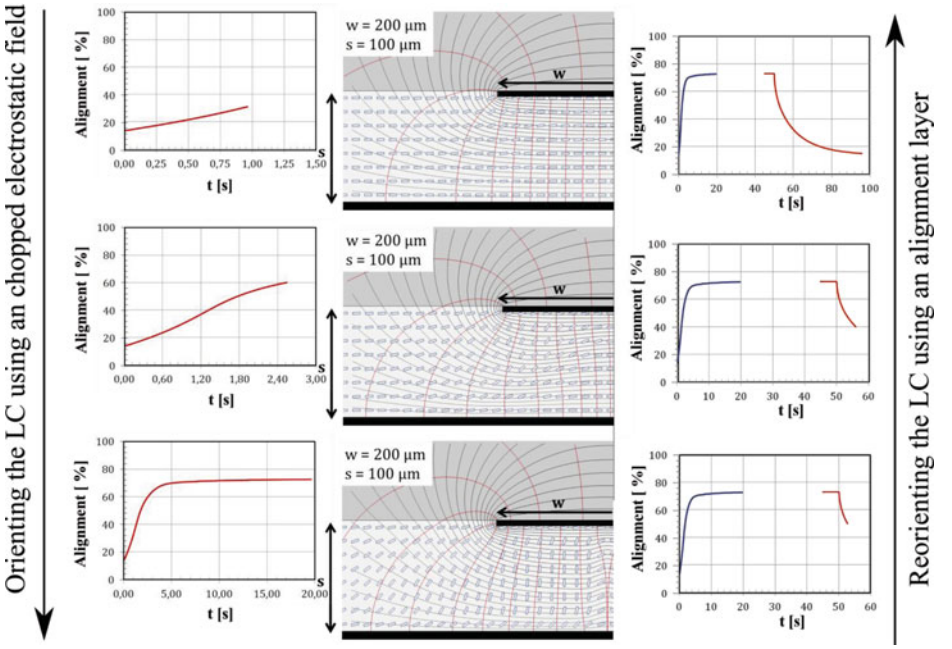

Figure 5. Flow chart of the director dynamic simulation of an inverted microstrip line containing (left) the time needed for the corresponding LC alignment using a chopped electrostatic field and (right) the time needed for the re-alignment using an alignment layer.

efficiency τ_φ of a device is defined as

$$\tau_\varphi = \frac{\Delta\varepsilon_{\text{eff}}}{\varepsilon_{\text{eff,max}} - \tau_{\text{LC}}}, \tag{15}$$

where $\Delta\varepsilon_{\text{eff}}$ is the difference of the unbiased and the biased - voltage controlled - state, $\varepsilon_{\text{eff,max}}$ is the highest obtained effective permittivity of the transmission line and τ_{LC} is the material tuneability of equation (2). The response time T_{10}^{90} defines the time, which is needed to orient the LC from one extreme state (e.g. perpendicular to the RF field) to the other extreme state (parallel to the RF field) and vice versa. An example for a detailed investigation of an LC based IMSL phase shifter at 30 GHz is shown in Figure 6.

An IMSL phase shifter with an LC layer height of 100 μm and a signal electrode width of 200 μm should exceed an *FoM* of 85° /dB according to the simulation, while having a tuning efficiency of approximately 74 %. The response time for LC reorientation only through means of the alignment layer is 36 s. Further investigations on this structure showed, that by exchanging the LC GT3 with TUD-566 (see Table 1) an *FoM* of more than 140° /dB and a tuning efficiency of 76 can be yield.

Another transmission line based phase shifter, the coplanar waveguide (CPW) with ground, has been investigated at 30 GHz as well (see Figure 7).

For a signal electrode width of $w = 200$ μm, an LC layer height of $s = 100$ μm, a gap of $g = 150$ μm between the signal electrode and the ground and a GT3-filling, the CPW with ground should exceed an *FoM* of about 67° /dB and a tuning efficiency of around 60 % according to the simulation. For this case, the CPW with ground has a lower performance

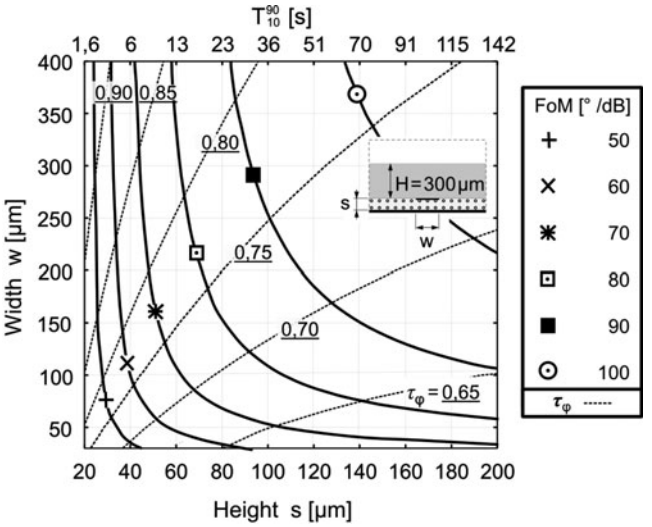

Figure 6. Figure of merit (*FoM*) and tuning efficiency τ_φ of an IMSL phase shifter filled with GT3 at 30 GHz as a function of the LC layer height *s* and signal electrode width *w*.

than the IMSL and it also needs more space due to the ground electrodes beside the signal electrode.

Nevertheless, these structures cannot exploit the full performance of the microwave optimized LC mixtures, due to the high metallic losses present in these comparatively planar structures. A hollow waveguide, which is known for its low metallic loss, will therefore reach a much better performance. Figure 8 shows the *FoM* and the length which is needed for an 360° phase shift depending on the frequency.

At 30 GHz the GT3 filled hollow waveguide exceeds an *FoM* of 110° /dB while needing a length of 55 mm to achieve a 360° phase shift. Using TUD-566 instead of GT3, an *FoM* of approximately 240° /dB can be reached, which would be 100° /dB more compared to

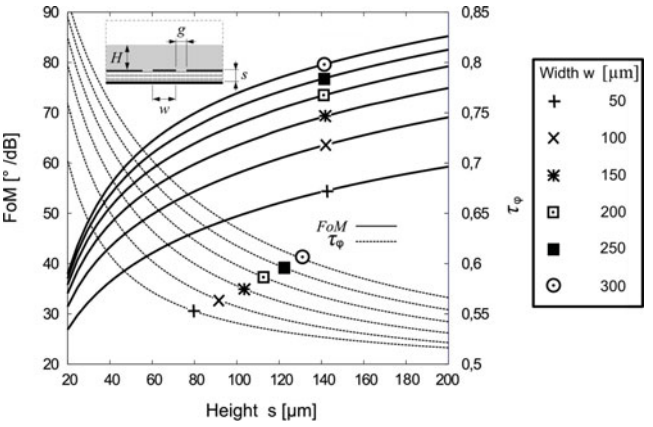

Figure 7. Figure of merit (*FoM*) and tuning efficiency τ_φ of a CPW with ground phase shifter filled with GT3 at 30 GHz as a function of the LC layer height *s* and signal electrode width *w*.

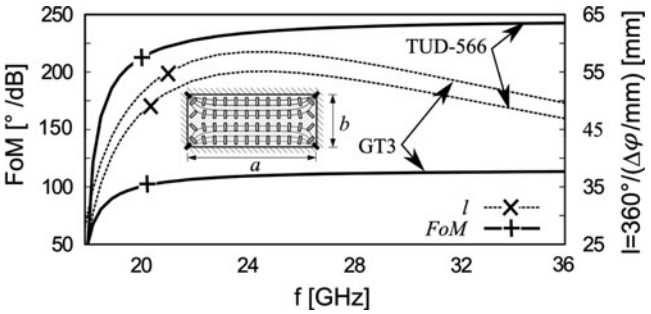

Figure 8. Frequency dependent *FoM* and minimum length *l* for a 360° phase shift for a hollow waveguide with dimensions $a = 5.0$ mm and $b = 2.0$ mm. The simulations were carried out for GT3 and TUD-566.

the IMSL filled with TUD-566. For achieving a phase shift of more than 360°, a length of approximately 52 mm is needed.

Therefore, the separation into two different categories, planar structured devices for mobile communication in cars or aircrafts and high performance devices for satellite communication, is reasonable. While the advantage of a hollow-waveguide based LC phase shifter is its high FoM, the planar structures benefit from the low response time of the LC due to the comparatively thin LC layer thicknesses.

Application of LC

As mentioned in the chapter above, LC-based phase shifters for phased array antennas is one key application for LCs in microwave engineering. As an example and even a proof of the applicability of LC at frequencies towards THz, a low loss hollow waveguide based LC phase shifter for W-band frequencies is shown [27]. The fabricated demonstrator is given in Figure 9.

The waveguide itself is designed in an u-shape. By inserting the LC container made of PTFE ($\varepsilon_r = 2.06$ and $tan\delta = 2.2 \cdot 10^{-4}$ at 100 GHz [28]) into the waveguide channel - as implied in Figure 9 (a) - and closing the splitblock with the top part, a press-fit sealing of the waveguide is achieved, due to the flexibility of the PTFE. This LC container is tapered in a triangular shape on both sides and has a LC cavity of 14.6 mm × 0.60 mm × 1.0 mm. A metallic tapering, two quarter-wave transformer steps for 100 GHz, have been implemented to ensure single mode propagation in the dielectric filled waveguide. After

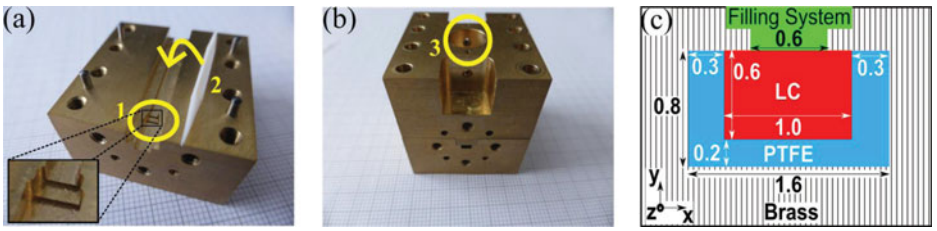

Figure 9. Images of (a) the splitblock bottom with -1- the u-shaped quarter-wave transformer steps and -2- the LC container made of PTFE, and (b) the assembled phase shifter including -3- the filling holes. In (c) a cross-section of the phase shifter is given (all length specifications in mm).

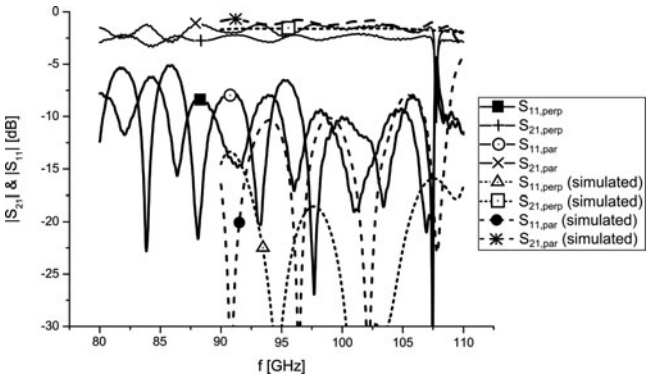

Figure 10. Measured (straight lines) and simulated (dashed lines) scattering parameters ($|S_{11}|$ & $|S_{21}|$) of the phase shifter.

sealing the waveguide it can be filled under normal conditions with LC using the two filling holes at the top, which can be closed from the side using copper register pins.

The measurements were carried out using an ANRITSU 37397C Vector Network Analyser (VNA) combined with two 3740A-EW extensions for frequencies in the extended W-band. The LC is aligned through permanent magnets and the results are shown in Figure 10.

The measured scattering parameters are almost consistent with the simulated ones, except the reflection coefficient for the perpendicular orientation, which is significantly higher than in the simulation. For the desired frequency range from 99 GHz – 105 GHz, for which the phase shifter is optimized, the return losses are better than 10 dB. The measured insertion losses show slightly higher values and a resonance at approximately 107 GHz, which is due to standing waves in the dielectric material. The insertion losses arise in general from the finite electrical conductivity of the brass, the dielectric losses of the PTFE, the dielectric losses of the LC and the losses due to a not perfectly closed split-block hollow waveguide. It is less than 2.7 dB in the desired frequency range.

The deviations between the simulated and measured results can be explained by manufacturing tolerances and the placing of the PTFE container. Since it is a flexible material, the triangular taper cannot be manufactured as precisely and symmetrically as in the simulation. Also the LC channel length was a bit shorter (14.6 mm instead of 15.0 mm). The quarter wave transformer steps are also not fabricated as ideally as in the simulation.

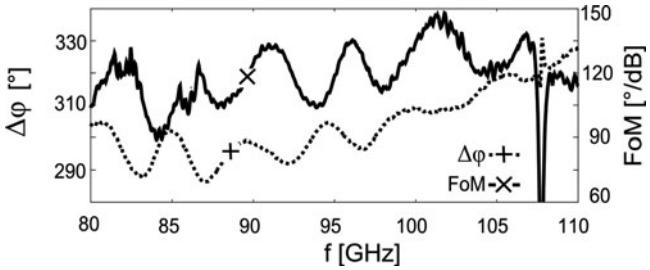

Figure 11. Differential phase shift $\Delta\varphi$ and figure of merit (*FoM*) of the W-band phase shifter, calculated out of the measured data.

The frequency dependent differential phase shift $\Delta\varphi$ and *FoM* are presented in Figure 11.

It exceeds a differential phase shift of 307° in the desired frequency range. This results in an *FoM* between 108° /dB – 148° /dB, which is, to the authors' knowledge, the highest value for passive phase shifters in this frequency range. The results are that rippled due to the standing waves inside the phase shifter.

Conclusion

During the last decade, LC mixtures have been optimized regarding tuneability and dielectric loss for the micro-, millimeter-wave and THz regime by using several characterisation setups. The state of the art characterisation setup is based on the dual mode cavity perturbation method mentioned above. The simulation tool *SimLCwg* allows the comparison of different LC based transmission line and waveguide structures in terms of figure of merit, tuneability and response time. With the help of this and other simulation tools like CST Microwave Studio®, several LC-based devices have been built for different applications, such as high performance phased array antennas for satellite communications. A record *FoM* of 200° /dB was demonstrated for a hollow-waveguide based LC phase shifter for Ka-band frequencies. Thanks to the constant values of the LC permittivity and dielectric loss over a wide frequency range, LC is a well-suited material for reconfigurable devices in the millimetre-wave and THz range, e.g. for beam-steering antennas for 5G-application. A hollow-waveguide based phase shifter for W-band frequencies shows an *FoM* up to 148° /dB. The results of this measurement are in a good agreement with the simulation.

Acknowledgments

The authors would like to thank Merck KGaA, Darmstadt, Germany for the provision of the LC material, CST AG, Darmstadt, Germany, for the support and LOEWE STT for providing the platform for this work.

References

[1] Yeh, P., & Gu, C. (2009). *Optics of Liquid Crystal Displays*, John Wiley & Sons, New Jersey, 2nd Edition.

[2] Stewart, I. W. (2004). *The Static and Dynamic Continuum Theory of Liquid Crystal: A Mathematical Introduction*, Taylor & Francis, London.

[3] Dolfi, D., Labeyrie, M., Joffre, P., & Huignard, J. P. (1993). *Electronics Letters*, *29*, 926–928.

[4] Weil, C., Luessem, G., & Jakoby, R. (2002). *IEEE MTT-S International Microwave Symposium Digest, 2002*, *1*, 367–371 vol.1.

[5] Borgioli, A., Yu Liu, Nagra, A. S., & York, R. A. (2000). *Microwave and Guided Wave Letters, IEEE*, *10*, 7–9.

[6] Mueller, S., Penirschke, A., Damm, C., Scheele, P., Wittek, M., Weil, C., & Jakoby, R. (2005). *Microwave Theory and Techniques, IEEE Transactions on*, *53*, 1937–1945.

[7] Mueller, S., Koeberle, M., Goelden, F., Penirschke, A., Gaebler, A., Lapanik, A., Haase, W., & Jakoby, R. (2008). *38th European Microwave Conference*, 119–122, 27-31 Oct.

[8] Penirschke, A., Muller, S., Scheele, P., Weil, C., Wittek, M., Hock, C., & Jakoby, R. (2004). *34th European Microwave Conference,* vol. 2, 545–548, 12-14 Oct.

[9] Gaebler, A., Goelden, F., Mueller, S., & Jakoby, R. (2008). *38th European Microwave Conference,* 909–912, 27-31 Oct.

[10] Weickhmann, C., Jakoby, R., Constable, E., & Lewis, R. A. (2013). *38th International Conference on Infrared, Millimeter, and Terahertz Waves*, 1–2, 1-6 Sept.
[11] Gaebler, A., Goelden, F., Mueller, S., & Jakoby, R. (2008). *AP-S IEEE*, 1–4.
[12] Müller, S. (2007). "Grundlegende Untersuchungen steuerbarer passiver Flüssigkristall-Komponenten für die Mikrowellentechnik." PhD thesis. Technische Universitaet Darmstadt.
[13] Gaebler, A., Goelden, F., Manabe, A., Goebel, M., Mueller, S., & Jakoby, R. (2009). *European Microwave Conference,* 594–597, Sept. 29-Oct. 1.
[14] Follmann, R., Kother, D., Campo, M. A., Franke, T., Gabler, A., Jakoby, R., Manabe, A., Rabe, T., Heunisch, A., Rauch, A., & Kasser, T. (2013). *IEEE-APS Topical Conference on Antennas and Propagation in Wireless Communications*, 90–93, 9-13 Sept.
[15] Hoehn, A., Hager, P. B., & Harder, J. T. (2013). *Aerospace Conference IEEE*, 1–14, 2-9 March.
[16] Bildik, S., Dieter, S., Fritzsch, C., Frei, M., Fischer, C., Menzel, W., & Jakoby, R. (2011). *41st European Microwave Conference*, 1292–1295, 10-13 Oct.
[17] Karabey, O. H., Gaebler, A., Strunck, S., & Jakoby, R. (2012). *IEEE Transactions on Microwave Theory and Techniques*, *60*, 1297–1306.
[18] Karabey, O. H., Bildik, S., Bausch, S., Strunck, S., Gaebler, A., & Jakoby, R. (2013). *IEEE Transactions on Antennas and Propagation*, *61*, 70–76.
[19] Strunck, S., Karabey, O. H., Gaebler, A., & Jakoby, R. (2012). *Electronics Letters*, *48*, 441–443.
[20] Weickhmann, C., Nathrath, N., Gehring, R., Gaebler, A., Jost, M. & Jakoby, R. (2013). *European Microwave Conference*, 428–431, 6-10 Oct.
[21] Shihe, L., Akyel, C., & Bosisio, R. G. (1981). *IEEE Transactions on Microwave Theory and Techniques*, *29*, 1041–1048.
[22] Brent, R. P. (1971). *The Computer Journal*, *14*, 422–425.
[23] Gaebler, A., Gölden, F., Müller, S. & Jakoby, R. (2008). *German Microwave Conference*.
[24] Gaebler, A., Gölden, F., Müller, S., & Jakoby, R. (2008). *Frequenz*, *9-10*, 240–245.
[25] Frank, F. C. (1958). *Discuss. Faraday Soc.*, *25*, 19–28.
[26] Stewart, I.W. (2004). *The Static and Dynamic Continuum Theory of Liquid Crystals: A Mathematical Introduction*, Taylor and Francis, London.
[27] Jost, M., Weickhmann, C., Strunck, S., Gaebler, A., Fritzsch, C., Karabey, O.H., & Jakoby, R. (2013). *Electronics Letters*, *49*, 1460–1462.
[28] Hirvonen, T. M., Vainikainen, P., Lozowski, A., & Raisanen, A.V. (1996). *IEEE Trans. Instrum. Meas. 45*, Aug., Nr. 4, S. 780–786.